Journal of Computer Science

Original Research Paper

Cooling Load Prediction in the Under-Actuated Zone with Multilayer Perceptron Artificial Neural Network

[1]Yaddarabullah, [2]Aedah Abd Rahman and [3]Amna Saad

[1]*Department of Informatics, Universitas Trilogi, Jakarta, Indonesia*
[2]*Schools of Science and Technology, Asia e University, Selangor, Malaysia*
[3]*Malaysian Institute of Information Technology, Universiti Kuala Lumpur, Kuala Lumpur, Malaysia*

Article history
Received: 22-09-2024
Revised: 29-10-2024
Accepted: 06-11-2024

Corresponding Author:
Yaddarabullah
Department of Informatics, Universitas Trilogi, Jakarta, Indonesia
Email: yaddarabullah@trilogi.ac.id

Abstract: This study focuses on addressing the challenge of predicting cooling loads in under-actuated zones, where the variability in occupant behavior, environmental conditions, and electronic usage creates complex dynamics. Traditional models like Support Vector Regression (SVR) and E-Lastic-Net (ELN) often struggle to capture these non-linear relationships, leading to inefficient Heating, Ventilation, and Air Conditioning (HVAC) management and increased energy consumption. To overcome this, the research proposes a hyperparameter-tuned Multi-Layer Perceptron-Artificial Neural Network (MLP-ANN) model, enhanced by integrating trainable bias and custom weight scaling. The results show that the proposed model significantly outperforms both baseline models and state-of-the-art techniques. The model using leaky ReLU with trainable bias and a weight scale of 2.0 achieved superior performance, with an RMSE of 128.26, MAE of 90.65, and an R^2 of 0.9992. In comparison, the baseline models demonstrated RMSE values between 1906 and 1919 and R^2 scores ranging from 0.8105-0.8141, showcasing the proposed model's effectiveness. Furthermore, activation function performance showed substantial improvement, particularly in reducing dead neurons and training loss. ReLU with trainable bias and a weight scale of 2.0 had a final training loss of 1,034,874.61 and 0.83% dead neurons, while PReLU and leaky ReLU with trainable bias had 0% dead neurons. These enhancements, along with improved smoothness scores (ranging from 0.84-1.24), contributed to more stable and accurate predictions, highlighting the benefits of trainable bias and custom weight scaling in improving model performance and generalization.

Keywords: Cooling Load, Under-Actuated HVAC Zone, Neural Network, Occupant Behavior, Time Interval

Introduction

In the realm of modern building design, the primary challenge remains the balance between energy efficiency and occupant comfort, with Heating, Ventilation, and Air Conditioning (HVAC) systems playing a pivotal role in maintaining indoor environmental quality. These systems are indispensable but also significant contributors to a building's overall energy consumption. Indoor climate control has categorized zones in buildings into two types: The "fully actuated" and the "under-actuated" zones (Brooks *et al*., 2015). A fully actuated zone is a space that can be independently controlled using dedicated HVAC equipment, making it suitable for environments where the number of occupants and their activities are well-defined, such as classrooms, offices, or auditoriums. Conversely, the under-actuated zone lacks an independent cooling or heating system and instead relies on the HVAC systems of adjacent zones. This type of zone is often found in spaces like lobbies, corridors, and other communal areas where the presence and behavior of occupants are difficult to predict (Kong *et al*., 2022).

Of particular interest within the field of HVAC is the cooling load, which measures the amount of heat that needs to be removed from a space to maintain optimal comfort. This load is influenced by multiple factors, including external weather conditions, building design, and occupant behavior. In under-actuated zones, cooling load control becomes particularly complex. The control systems in such zones typically rely on the averaged

cooling load data across multiple rooms, leading to inefficiencies and poor indoor climate control (Brooks *et al*., 2015). The challenge is exacerbated when climate conditions vary between areas within the under-actuated zone, resulting in varied cooling loads in different ventilation areas at any given time. This variability is primarily caused by the presence and activities of occupants in these spaces (Yang and Becerik-Gerber, 2016). Additionally, the dynamic and temporal variability of occupancy-driven cooling loads further complicates the development of uniform cooling strategies across different areas and times (Wang *et al*., 2018; Yaddarabullah *et al*., 2023). The resultant lack of proper control can adversely affect occupant comfort and health, as thermal conditions deviate from the desired range.

The literature has extensively explored methods to analyze occupant behavior in efforts to optimize HVAC systems in under-actuated zones. Approaches have included mathematical models, dimensional models, statistical models, simulation models, and deep learning models. The ASHRAE standard no. 55 provides a mathematical framework for calculating cooling loads based on occupancy, accounting for the number of occupants and their activities (Ghaffari Jabbari *et al*., 2020). Occupant-centric control (OCC) models were introduced to capture interactive dimensions of occupant characteristics, leveraging real-time data from target buildings to assess factors such as occupancy presence, activities, and electrical appliance usage (Yan *et al*., 2015; Yang *et al*., 2022). Statistical approaches, such as Markov Chains and Survival Analysis, have been used to model occupant behavior patterns, with Markov Chains capturing transitions between different rooms and behaviors and Survival Analysis identifying temporal patterns in occupant activities (Wang *et al*., 2018; Zhao *et al*., 2022).

However, these traditional models whether mathematical, dimensional, or statistical face notable limitations in the context of under-actuated zones. Mathematical models, such as those conforming to ASHRAE standards, tend to oversimplify occupant behavior, failing to capture the dynamic and variable nature of human interactions with indoor environments (Ahmed *et al*., 2023). Additionally, these models rely heavily on static parameters and are unable to adapt to real-time changes, thereby limiting their applicability in unpredictable environments (Kim and Cho, 2022). Statistical models like Markov Chains and Survival Analysis, while useful for specific applications, often require extensive data collection, rendering them costly and resource-intensive. Moreover, they operate under strict assumptions about probability distributions and event independence, which may not always hold, leading to overfitting and poor generalization of new data (Hussein *et al*., 2023).

Simulation models offer another avenue for cooling load analysis, wherein engineers use simulation software to replicate building design scenarios and estimate energy demands. These simulations are often accurate, mirroring real-world observations (Sholahudin and Han, 2016). However, their applicability is limited by the time-consuming nature of the simulations and the need for expert operators. In contrast, deep learning models have emerged as a promising alternative for predicting cooling loads. A study by Kim *et al*. (2020) demonstrated that predictive models, particularly those leveraging deep learning, outperform traditional simulation methods by providing more efficient and accurate cooling load predictions. By utilizing historical data and advanced learning algorithms, deep learning models offer a viable pathway for optimizing HVAC systems, particularly in dynamic environments like under-actuated zones (Gao *et al*., 2021; Moradzadeh *et al*., 2022).

The use of deep learning models, particularly the Multi-Layer Perceptron-Artificial Neural Network (MLP-ANN), for cooling load prediction has gained traction in recent years. Moradzadeh *et al*. (2022) highlighted the effectiveness of MLP-ANN models and Support Vector Regression (SVR) in developing nonlinear models for cooling load prediction. However, these methods are not without challenges. The performance of SVR models is highly sensitive to kernel selection and hyperparameter tuning, while MLP-ANN models require careful attention to network architecture and learning algorithms to ensure effective model training (Al-Shargabi *et al*., 2021). Crucial to the success of these models is the interaction between input features and the choice of activation functions, both of which significantly influence model performance. While ReLU is a popular activation function, it is susceptible to the "dying ReLU" problem, where neurons become inactive, impeding model learning, particularly in datasets with complex feature interactions (Kulathunga *et al*., 2021).

To overcome these limitations, the present study introduces modified activation functions, including bias terms, and explores alternative weight initialization strategies such as Glorot Uniform, which have been shown to enhance model performance (Olimov *et al*., 2021; Yang *et al*., 2023). By integrating bias terms into the activation functions, the model can shift activation thresholds, helping to mitigate issues like the dying ReLU problem. This, combined with careful hyperparameter tuning and feature engineering, enables the MLP-ANN model to better capture the complex dynamics of occupant-driven cooling loads in under-actuated zones.

This study focuses on the cooling load driven by occupant behavior in the student corner of the library at Universitas Trilogi, an under-actuated zone. Data were collected following ASHRAE standard no. 55, with variables recorded every 5 min from Monday-Friday, 8 am-4 pm, over a 14-week period. These variables include occupant presence, number, activities, and appliance usage,

which contribute to internal heat gain within the zone. A polynomial regression approach was employed to analyze the time intervals of cooling load based on occupancy patterns, leading to the development of a cooling load prediction model using MLP-ANN. The study also implemented rigorous data preprocessing, including feature selection, validation, and reliability analysis, ensuring that only the most relevant data were used for model training. By optimizing hyperparameters and integrating custom activation functions, this research aims to enhance the adaptability and accuracy of cooling load predictions in under-actuated zones, offering a pathway towards more energy-efficient and occupant-friendly HVAC systems.

Related Work

Machine Learning (ML) has emerged as a powerful tool in predicting cooling loads based on occupancy, enabling the optimization of energy efficiency within residential buildings. Several studies have showcased state-of-the-art ML applications for forecasting cooling loads, yet they have not adequately addressed the complexities inherent in under-actuated zones, where cooling requirements vary across different areas and times. Furthermore, these studies have largely overlooked the critical aspect of determining the appropriate time intervals for each zone across different days, a factor that plays a crucial role in ensuring accurate and effective cooling load management.

Sha *et al*. (2021) applied nine different ML techniques, including E-Lastic Net (ELN), Support Vector Regression (SVR), Gradient Tree Boosting (GTB) and Multi-Layer Perceptron-based-Artificial Neural Network (MLP-ANN), to predict cooling loads. Their models were trained using data from the Building Automation System (BAS), recorded at three distinct time intervals: 6, 30 min, and 1 h. While GTB emerged as the most effective technique, with the lowest Root Mean Square Error (RMSE) and Normalized Mean Bias Error (NMBE) scores, this study did not account for the cooling loads in individual zones within the building. Instead, it focused on the building as a whole, ignoring the potential variability between different areas. Additionally, the study did not explore optimal time intervals for predicting cooling loads, which could significantly enhance the model's accuracy and applicability in zone-specific environments. The models primarily relied on the Rectified Linear Unit (ReLU) activation function, which, while widely used, may not capture the intricate patterns and non-linearities present in real-world data across multiple zones.

Similarly, Fan *et al*. (2017) conducted research on advanced data analytics for cooling load prediction using deep learning algorithms, such as Multiple Linear Regression (MLR), E-Lastic Net (ELN), and Support Vector Regression (SVR). Their study emphasized the importance of feature extraction to enhance model performance, reducing the dimensionality of the inputs. The dataset included both historical and real-time data, recorded at one-h intervals. The study identified Extreme Gradient Boosting (XGB) as the best-performing model, with the lowest RMSE score. Despite these findings, this research was limited to a single area and did not account for the time intervals necessary for zone-specific cooling load predictions. Furthermore, the exclusive use of ReLU as the activation function limited the model's ability to capture complex, non-linear behaviors in occupant activities and environmental changes, thereby reducing its effectiveness in predicting cooling loads in under-actuated zones with varying conditions.

Guo *et al*. (2023) proposed a cooling load prediction model that combined LightGBM with hyperparametric optimization methods, such as the Covariance Matrix Adaptive-Evolution Strategy (CMA-ES) and the Tree-structured Parzen Estimator (TPE). Their study compared several hyperparameter tuning techniques, concluding that the TPE-LightGBM model offered the best performance in terms of RMSE, MAE, and R^2. However, like previous research, Guo *et al*., study focused solely on a single area and did not consider the variability in cooling loads across different zones or the significance of selecting appropriate time intervals for each zone. The neglect of these factors diminishes the model's applicability in dynamic environments where cooling requirements fluctuate based on occupant behavior and environmental conditions. Furthermore, although the model's performance was enhanced through hyperparameter tuning, it still failed to address the non-linear complexity and temporal patterns that are critical in accurately predicting cooling loads in under-actuated zones.

In a related study, Moradzadeh *et al*. (2022) examined a variety of neural network algorithms and regression techniques for cooling load prediction, including General Regression Neural Networks (GRNN), Group Method of Data Handling (GMDH), and Group Support Vector Regression (GSVR). The study found that GSVR, a hybrid of GMDH and SVR, outperformed other models in terms of R-value and prediction accuracy. Nevertheless, the study did not incorporate zone-specific cooling load predictions, nor did it consider the appropriate time intervals necessary for accurately forecasting cooling loads in under-actuated zones. Additionally, the use of a sigmoid activation function introduced the risk of vanishing gradients, which could hinder the model's ability to learn complex patterns in the data, particularly in dynamic and multi-zoned environments. The failure to address these critical aspects further limits the practical application of the proposed models in real-world settings, where occupant behavior and environmental conditions vary significantly across different zones and times.

Li and Yao (2020) conducted a comprehensive investigation into the prediction of residential heating and

cooling loads using various machine learning models, including linear and polynomial kernel Support Vector Regression (SVR) and Artificial Neural Networks (ANN). The study demonstrated that both the ANN and GRBF-SVR models were highly effective, achieving high levels of prediction accuracy in terms of MAE and RMSE. However, the research did not account for the variability of cooling loads across different zones within a building, nor did it explore the optimal time intervals for each zone. By focusing on the building as a whole, the study overlooked the nuanced patterns of occupant behavior that can impact cooling requirements in different areas. Furthermore, the linear activation function employed in the study may not have been sufficient to capture the complex, non-linear interactions between the variables, limiting the model's applicability in more complex, dynamic environments.

In summary, while these studies have advanced the field of cooling load prediction using machine learning techniques, they share common limitations that hinder their application in under-actuated zones. None of the studies addressed the critical aspect of determining appropriate time intervals for predicting cooling loads in different zones, nor did they fully account for the dynamic and non-linear patterns associated with occupant behavior.

Materials and Methods

Case Study

The research was conducted at the Universitas Trilogi Library, which encompasses both fully and under-actuated zones. As depicted in Fig. (1), the library has a total area of 628 square meters and is divided into seven distinct rooms. In this study, the term "zone" refers to a specific coverage area defined by the ceiling ventilation system, which is essential for maintaining consistent air distribution and temperature regulation within each designated space. Additionally, "room" refers to the larger segmented areas within the library that may contain one or more zones. Rooms 1, 2, and 6 are classified as fully actuated zones, where the HVAC system is optimized to dynamically adjust airflow and temperature based on real-time occupancy and environmental conditions. In contrast, Rooms 3, 4, 5, and 7 are under-actuated zones, characterized by less sophisticated control mechanisms and reliance on static, predetermined settings.

The library's climate control system consists of a main chiller unit housed in the energy station, equipped with an Air Handling Unit (AHU) boasting a cooling capacity of 10,000 kW. This system utilizes a single main duct from the AHU, which distributes air through 23 vents servicing the four under-actuated HVAC zones and 4 vents servicing the four fully actuated HVAC zones. The research focuses on Room 3, known as the student corner, which comprises three distinct ventilation zones of approximately 25 square meters each. These zones are equipped with ceiling ventilation systems designed to manage airflow and temperature, thereby maintaining a controlled environment for occupants. Given the occupied capacity of 40 persons, effective HVAC management in the student corner is essential for both comfort and energy efficiency.

Thermal Preferences

Thermal preferences for various occupant activities, as outlined in Table (1), are based on the sensible heat gain values specified by ANSI/ASHRAE standard no. 55, 2010. These values are expressed in Watts per square meter (W/m²), demonstrating the differences in heat transfer depending on the type and intensity of the activity. For example, activities such as sitting, standing, or walking have distinct thermal outputs that impact the overall thermal comfort of occupants within a space. The heat transfer for an average occupant is 73.25 watts, which is approximately equivalent to 250 Btu/h.

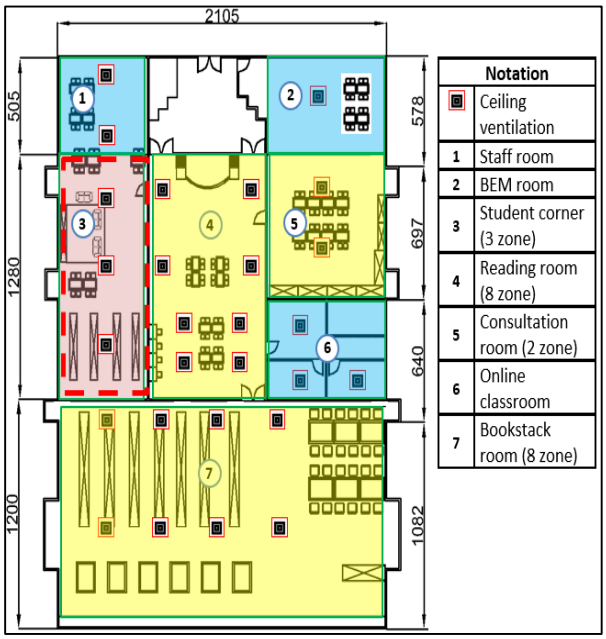

Fig. 1: Layout of Universitas Trilogi Library

Table 1: Thermal preferences of occupant activity

No	Type of Activity	Watt/m2
1	Stand	70
2	Sit	60
3	Walk	100
4	Squat	60
5	Talk	70
6	Write	60
7	Sleep	40
8	Typing	60
9	Light activity	67

Table 2: Thermal preferences of electronic usage

No	Type of appliance operation	Watt/m2
1	Use a laptop or computer	50
2	Use handphone	4
3	Use headset	0,5

Each electronic device utilized by the occupants during their activities possesses a distinct heat transfer coefficient that characterizes the quantity of heat produced by the device. Table (2) displays the coefficients based on the power consumption of each electronic device and serves as a reference for gauging the heat transfer.

Data Collection

Data were gathered from three distinct regions (Zone 1-3) within an office setting during regular working h (8 am to 4 pm) on weekdays. Data was systematically collected throughout an academic semester, chosen due to the continuous nature of campus activities over a typical 14-week period. The data collection schedule was meticulously aligned with the standard academic timetable. A mixed-methods approach, incorporating both manual and automated techniques, was employed to ensure a robust and comprehensive dataset.

Manual data collection entailed direct observation, whereby the number of occupants, their activities, and their use of electronic devices were meticulously recorded through the analysis of CCTV footage. Automated data collection methods were facilitated by an array of sensors and monitoring systems, which captured data on environmental conditions and occupant behavior. This dual-methodological approach enhanced the validity of the data, contributing to the reliability of the study's findings. The recorded occupant behavior was subsequently quantified for its impact on cooling load, using a designated formula, and integrated into the occupant dataset, which included metrics on occupant number load, activity load, and electronic usage load.

Data pertaining to external and internal loads, such as environmental conditions and HVAC performance, was collected via a network of indoor and outdoor sensors measuring air pressure, temperature, and relative humidity. This automatically captured data was initially acquired in JSON format through an Internet of Things (IoT) server and subsequently converted into CSV format. The resulting compiled dataset was stored in CSV format and later updated with computed cooling load values derived from the designated formula.

Cooling Load Measurement

Cooling load refers to the rate at which both sensible and latent heat must be extracted from an indoor space to maintain a desired temperature and humidity level, ensuring thermal comfort for occupants. The primary aim of cooling load measurement is to determine the required capacity of air conditioning and refrigeration equipment to sustain acceptable interior conditions during periods of high external temperatures (Hashim *et al*., 2018). It plays a critical role in designing efficient HVAC systems, as the cooling load directly influences the size and operation of these systems. The cooling load consists of two main components: Sensible heat load and latent heat load, both of which are essential in determining the overall thermal performance of a building (Bathia, 2014).

The sensible heat load pertains to the change in the dry bulb temperature of the indoor environment and is influenced by factors such as heat gain from external sources (e.g., solar radiation, conduction through walls and windows) and internal sources (e.g., occupants, lighting, and equipment). This heat load affects the air temperature, which the HVAC system must reduce to achieve the desired comfort level. On the other hand, the latent heat load refers to the moisture content within the conditioned space, which arises from sources like human respiration, evaporation from wet surfaces, and infiltration of humid outside air. This component influences the humidity level in the space and requires dehumidification to maintain an optimal indoor environment. Together, the sensible and latent loads define the total cooling load on a building, shaping the overall demand for cooling energy.

Occupant load, a significant part of the total cooling load, is based on factors such as the number of occupants, the total h they spend in the space, the types of activities they engage in, and the extent of electronic device usage (Wang *et al*., 2018). Occupants generate both sensible and latent heat, contributing to the thermal load through their metabolic activities and the operation of electronic devices. For instance, higher metabolic activities like walking or exercising generate more heat compared to sedentary activities such as sitting or reading. Similarly, the use of electronic devices like computers and mobile phones adds to the heat load, further influencing the cooling requirements of the space.

The sensible and latent loads generated by occupants can be quantified using a mathematical equation, which combines the heat from activities (Q_{Act}) and the heat from electronic device usage (Q_{ED}). The total occupant load (Q) can thus be expressed as:

$$Q = Q_{Act} + Q_{ED} \quad (1)$$

In this equation, Q_{Act} represents the total sensible and latent heat generated by the occupants based on their activities, as outlined in Table (1), where each type of activity has a corresponding heat output in Watts per square meter (W/m²). For example, walking generates 100 W/m², whereas sitting produces 60 W/m². Q_{ED} on the other hand, accounts for the heat produced by electronic device usage, as shown in Table (2). Devices such as laptops contribute 50 W/m², while mobile phones contribute 4 W/m².

Time Interval Measurement

Polynomial regression was utilized to determine the appropriate time period for each zone-based occupancy

(Wang *et al*., 2018). This technique reveals the pattern of data changes that occur within a specific time unit. By reorganizing the dataset format, a representative dataset with varying cooling load needs can be produced. Polynomial regression is a form of linear regression where only due to the non-linear relationship between dependent and independent variables (Sagar *et al*., 2021). In polynomial regression, the relationship between the dependent variable and the independent variable is modeled as an in-degree polynomial function. For a polynomial of degree 2, the relationship is referred to as a quadratic model and the equation is given by:

$$y = \beta_0 + \beta_1 x + \beta_2 x^2 + \epsilon \quad (2)$$

where:

- y is the dependent variable
- x is the independent variable
- $\beta 0$, $\beta 1$, $\beta 2$ are the coefficients
- ϵ is the error term

Features Selection Based on Validity and Reliability

Features selection was guided by both validity and reliability measures to ensure a robust dataset. The validity of the data was established through the application of Exploratory Factor Analysis (EFA), which identified underlying relationships among variables without imposing a predefined structure. Low-variance variables (less than 0.1) were eliminated, as they demonstrated minimal variability across the dataset, indicating that they remained relatively stable under different conditions or over time (Watkins, 2018).

A factor loadings heatmap was utilized to visualize the relationships between variables and the extracted factors. This helped determine the optimal number of factors needed to capture the underlying structure of the data. A correlation matrix was then generated to assess the interrelationships among the selected features, focusing on highly correlated pairs (correlation >0.8 or <-0.8) (Zhang *et al*., 2020). Insights from the factor loadings and correlation matrix helped refine the feature selection process, ensuring that the remaining features were both meaningful and representative.

To further ensure the reliability of the selected features, test-retest reliability was conducted by comparing measurements taken at different intervals. A high Pearson correlation coefficient (typically exceeding 0.7) confirmed strong temporal stability, indicating that the dataset consistently produced reliable results over repeated measurements. Moderate reliability values, ranging from 0.6-0.7, were also deemed acceptable, reflecting a reasonable degree of stability over time (Lee *et al*., 2018). These combined analyses ensured that the final set of features was both valid and reliable, providing a solid foundation for the study's findings.

Feature Engineering

A comprehensive feature engineering process was undertaken to enhance the predictive accuracy of the cooling load prediction model. Various transformations and constructions were applied to the dataset to enrich its predictive power and provide deeper insights into the temporal and contextual relationships affecting cooling load.

Sine and cosine transformations were applied to capture the cyclical nature of the temporal variables. The month variable was transformed into its sine (month-sin) and cosine (month-cos) components, effectively encoding the seasonal periodicity within the year. Similarly, the week and day variables were transformed using sine and cosine functions to retain their cyclical patterns across weeks and days. These transformations allowed the model to better recognize and leverage the repetitive temporal cycles, thereby improving its ability to predict cooling loads based on seasonal variations and daily or weekly patterns (Kim and McMahon, 2021).

Lag features were introduced to incorporate historical cooling load values, which provided the model with information about recent cooling load trends. By including the cooling load from one and two-time steps prior (cooling-load-lag-1 and cooling-load-lag-2), the model was able to detect temporal dependencies, enabling it to predict future values with greater accuracy. The introduction of lagged values helped the model account for temporal autocorrelation and trends (Kamińska *et al*., 2020), key factors in predicting cooling loads in dynamic environments. The lagged cooling load values were calculated as:

$$cooling\_load\_lag\_1 = cooling\_load_{t-1} \quad (3)$$

$$cooling\_load\_lag\_2 = cooling\_load_{t-2} \quad (4)$$

Rolling statistics were also computed to capture local trends and variability in the cooling load data. A rolling mean was calculated over a three-time step window, providing a smoothed version of the data and helping the model identify long-term trends while reducing short-term noise. Similarly, the rolling standard deviation measured the variability within this window, highlighting periods of high or low volatility. These rolling features allowed the model to account for shifts in data patterns and periods of instability (Li *et al*., 2023; Ruddell *et al*., 2014; Sultana *et al*., 2019). The rolling mean and standard deviation were calculated over a three-time step window as follows:

$$Rolling\_mean = \frac{1}{3} \sum_{i=t-2}^{t} cooling\_load_i \quad (5)$$

$$Rolling\_std = \sqrt{\frac{\sum_{i=t-2}^{t} (cooling\_load_i - rolling\_mean)^2}{3}} \quad (6)$$

Time interval features were critical in accounting for the varying time intervals observed across different zones and days of the week. The time interval variable, recorded as the number of min (e.g., 30 or 60 min), provided essential information about the temporal granularity of the data (Kuiper and Ryan, 2018). Time interval features, based on the zone and day of the week, were also included to reflect the varying time intervals in different zones. The interaction term:

$$Interaction = zone \times time\_interval \times day \quad (7)$$

Finally, the original temporal variables such as the day of the week, week of the year, and month of the year were retained to provide additional temporal context.

Feature Dataset

The variables in the dataset (features) comprise two categories: Input variables and output variables. There are a total of 25 original variables and 15 from feature engineering, where the input variables number 40. The input variables include information about the date, time, and number of occupants, as well as details regarding the activity, electronic usage, and environmental conditions. The output variable represents the cooling load, which is expressed in numerical form. A more comprehensive description of the variables in the dataset can be found in Table (3).

Table 3: Dataset features with feature engineering

Features	Description
Num-occupant	Represents the total number of occupants within a zone at a given time. This variable is critical for understanding the overall occupancy pattern and its impact on cooling requirements
Num-stand	Denotes the number of individuals standing in the zone. Standing occupants may increase heat output, affecting the cooling load
Num-sit	Identifies the number of individuals sitting in the zone. Sitting is typically associated with lower metabolic rates, which may influence the cooling load
Num-walk	Captures the number of occupants walking within the zone. Walking activity generates higher metabolic heat, directly impacting cooling demands
Num-squat	Indicates the number of individuals squatting in the zone, a posture that might affect both metabolic heat and spatial arrangement
Num-read	Quantifies the number of occupants engaged in reading activities. Reading is a sedentary activity, with a relatively low influence on metabolic heat generation
Num-talk	Reflects the number of occupants talking, which may produce additional heat due to increased physical exertion from vocalization
Num-write	Tracks the number of individuals writing, a sedentary activity similar to reading, with low heat generation
Num-sleep	Records the number of individuals sleeping in the zone, which represents minimal physical activity and heat generation
Num-typing	Denotes the number of individuals engaged in typing on computers or other devices, contributing marginally to the heat load through both the activity and the use of electronic devices
Num-light-work	Describes the number of occupants involved in light work, an activity category that generates moderate heat compared to sedentary activities
Num-headphone	Captures the number of individuals using headphones, which may indirectly impact the cooling load by reducing movement or changing occupant behavior
Num-mobile phone	Identifies the number of individuals using mobile phones. Mobile device usage may slightly influence heat generation through device operation and user movement
Num-computer	Indicates the number of individuals using computers in the zone, which contributes both directly (through device heat output) and indirectly (through occupant behavior) to the cooling load
Indoor-temp	Measures the ambient temperature inside the monitored zone. Indoor temperature is a critical determinant in assessing cooling load requirements
Indoor-hum	Represents the relative humidity inside the monitored zone. Humidity levels directly affect occupant comfort and the efficiency of cooling systems
Indoor-air-pressure	Reflects the air pressure inside the zone, an important factor in HVAC system performance and occupant comfort
outdoor-temp	Records the temperature outside the monitored zone. Outdoor temperature influences the internal cooling load by affecting the heat exchange between indoor and outdoor environments
Outdoor-hum	Captures the relative humidity outside the monitored zone, impacting cooling strategies and HVAC system operation
Outdoor-air-pressure	Indicates the air pressure outside the zone, which may influence air exchange rates and consequently, cooling demands
Month-sin Month-cos	These are periodic transformations (using sine and cosine) to represent the month of the year, capturing seasonal variation patterns without introducing discontinuities
Week-sin Week-cos	Similar transformations are applied to represent the week of the year in a cyclical form, ensuring a smooth representation of temporal trends
Day-sin Day-cos time	Cyclical transformations of the day of the week, used to model weekly patterns without abrupt transitions between days
interval-category	Categorizes the time intervals between observations, facilitating analysis of time-dependent effects on cooling loads

Features	Description
Cooling-load-lag-1 Cooling-load-lag-2	Represent the cooling load from previous time steps (lagged by 1 and 2 intervals), included to capture autocorrelation and temporal dependencies in cooling load dynamics
Rolling-mean	Calculates the rolling mean of the cooling load over a specified window, helping smooth short-term fluctuations and reveal underlying trends
Rolling-std	Measures the rolling standard deviation of the cooling load, capturing the variability within the specified window
Zone-time-interval-interaction	Models the interaction between the specific zone and the time interval, capturing the unique cooling load patterns associated with different zones over varying intervals
Zone-day-interaction	Represents the interaction between the zone and the day of the week, accounting for potential variations in cooling load patterns across zones on different days
Time-interval-day-interaction	Captures the interaction between the time interval and the day of the week, modeling potential temporal variations in cooling load patterns
Zone-time-interval-day-interaction	Represents the combined interaction of zone, time interval, and day of the week, allowing for the most granular analysis of cooling load patterns across different zones, intervals, and days
Cooling-load	The total cooling load required to maintain the desired conditions within the monitored zone

Table 4: Set parameter for the baseline model

Parameter	1st model	2nd model	3rd model
Neurons in 1st hidden layer	Min = 32, max = 128	Min = 32, max = 128	Min = 32, max = 128
Dropout rate in 1st hidden layer	Min = 0.0, max = 2.0	Min = 0.0, max = 2.0	Min = 0.0, max = 2.0
Learning rate	Min = 1e-4, max = 1e-2	Min = 1e-4, max = 1e-2	Min = 1e-4, max = 1e-2
Activation function	ReLU	PReLU	Leaky ReLU
Weight initialization	Standard Glorot Uniform	Standard Glorot Uniform	Standard Glorot Uniform
Batch size	32	32	32
Iteration	50	50	50
Training and optimizer	Adam	Adam	Adam
Epoch	100	100	100
Cross-validation	10	10	10

Baseline Model of Cooling Load Prediction

The experiments of the baseline model were conducted using a Multi-Layer Perceptron-Artificial Neural Network (MLP-ANN) with one hidden layer. Two versions of the dataset were employed for this investigation: The original dataset without feature engineering and a feature-engineered version. The primary aim was to evaluate the influence of feature engineering and optimized hyperparameters on model performance. The experimental process began by establishing a baseline model for each dataset version, followed by a thorough hyperparameter tuning process to maximize model performance. The tuning process involved the use of several activation functions, including ReLU, leaky ReLU, and PReLU, along with their corresponding custom activation functions incorporating bias.

Hyperparameter tuning was conducted through random search, which involved sampling random combinations of hyperparameters from predefined ranges and evaluating their performance (Japa *et al*., 2023). The key hyperparameters adjusted in this process included the number of neurons in the hidden layer(s), the learning rate, the batch size, and the dropout rate. The study sought to identify the optimal settings that would yield the best model performance. The hyperparameters tuned in this study encompassed the number of neurons in both the first and second hidden layers, dropout rates for each hidden layer, and the learning rate. The tuning process was repeated 30 times to ensure a comprehensive exploration of potential configurations, thereby maximizing the likelihood of identifying the optimal settings. Table (4) presents the hyperparameter tuning strategy for a model with one hidden layer.

Custom of Weight Initialization

A custom weight initialization method was developed based on the GlorotUniform initialization to enhance the performance of the neural network model. The custom initializer was designed to scale the initialization process to better suit the specific requirements of the model architecture. The initializer was constructed by defining a class that inherits from tf.keras.initializers. Initializer, with an adjustable scale parameter to fine-tune the range of the initialized weights. The limit for the uniform distribution is computed using the formula derived from the GlorotUniform initialization. Specifically, the number of input units (fan-in) and the number of output units (fan-out) are determined based on the shape of the weight tensor. The limit is calculated as:

$$limit = scale \times \sqrt{\frac{6.0}{fan\_in + fan\_out}} \quad (8)$$

The scale parameter provides additional flexibility in determining the range of the weight initialization, allowing for better control over the distribution of weights in the network. The limit, determined by the chosen scale, defines the boundaries within which the weights are initialized. Specifically, the weights are drawn from a

uniform distribution within the interval defined by the limit. Mathematically, this can be expressed as:

$$W \sim Uniform(-limit, limit) \quad (9)$$

where, W denotes the weight matrix and the limit is calculated based on the scale parameter. This ensures that the weights are uniformly distributed within the range [-limit, limit], providing an effective initialization that supports faster convergence and improves model training.

Custom of Activation Function

ReLU with Bias

The ReLU with bias activation function modifies the standard ReLU function by adding a trainable bias term to the inputs before applying the ReLU operation. This function is defined as:

$$ReLUWithBias(x) = \max(0, x + bias) \quad (10)$$

where, x represents the input tensor and bias is a learnable parameter initialized to zero. By including the bias term, the activation function can shift the activation threshold, providing the model with additional flexibility to capture complex patterns in the data.

Leaky ReLU with Bias

The Leaky ReLU with bias activation function extends the traditional Leaky ReLU by adding a bias term to the inputs. The Leaky ReLU function is characterized by allowing a small, non-zero gradient when the input is negative. The modified function is defined as:

$$L.ReLUBias(x) = max(\alpha(x + bias), x + bias) \quad (11)$$

where, α is a predefined slope for the negative part of the function and bias is a trainable parameter. This adjustment enables the model to maintain gradient flow even for negative inputs while providing the flexibility to adjust the activation threshold.

PReLU with Bias

The PReLU with bias activation function builds upon the PReLU (Parametric ReLU) by incorporating both a trainable slope parameter (α) and a bias term. This activation function is defined as:

$$PReLUBias(x) = max(\alpha . (x + bias), x + bias) \quad (12)$$

where, both α and bias are trainable parameters. The inclusion of these parameters allows the model to learn the optimal shape of the activation function for different regions of the input space.

Proposed Model of Cooling Load Prediction

For the proposed models, as shown in Table (5), the hyperparameters tuned included similar ranges for the number of neurons in the first hidden layer, the dropout rate, and the learning rate. Custom activation functions with bias ReLU with bias, PReLU with bias, and leaky ReLU with bias were utilized to provide the models with additional flexibility. A custom GlorotUniform initialization with varying scales (0.5, 1.0, 1.5, and 2.0) was applied for weight initialization. These models were also trained with a batch size of 32 for 100 epochs, using the Adam optimizer. The random search method was employed for hyperparameter tuning, with 50 iterations conducted for each configuration. Cross-validation with ten folds ensured assessment of model performance.

Model Evaluation

The evaluation of the MLP-ANN prediction model's performance was carried out using three key metrics: Root Mean Squared Error (RMSE), Mean Absolute Error (MAE), and the coefficient of determination (R^2). These metrics were chosen to offer a comprehensive assessment of the model's prediction accuracy, error magnitude, and ability to account for variations in airflow volume changes within under-actuated zones. *RMSE*, widely used for measuring prediction errors (Zhang, 2024), represents the average magnitude of those errors and is defined mathematically as:

$$RMSE = \sqrt{\frac{1}{n}} \sum_{i=1}^{n} (y_i - \hat{y_i})^2 \quad (13)$$

Table 5: Set parameter for the proposed model

Parameter	1st model	2nd model	3rd model
Neuron in 1st hidden layer	Min = 32, Max = 128	Min = 32, Max = 128	Min = 32, Max = 128
Dropout rate in 1st hidden layer	Min = 0.0, Max = 2.0	Min = 0.0, Max = 2.0	Min = 0.0, Max = 2.0
Learning rate	Min = 1e-4, Max = 1e-2	Min = 1e-4, Max = 1e-2	Min = 1e-4, Max = 1e-2
Activation function	ReLU with bias	PreLU with bias	Leaky ReLU with bias
Weight initialization	Custom Glorot Uniform with scale (0.5, 1.0, 1.5, 2.0)	Custom Glorot Uniform with scale (0.5, 1.0, 1.5, 2.0)	Custom Glorot Uniform with scale (0.5, 1.0, 1.5, 2.0)
Batch size	32	32	32
Iteration	50	50	50
Training and optimizer	Adam	Adam	Adam
Epoch	100	100	100
Cross-validation	10	10	10

The Mean Absolute Error (MAE) was applied to assess the average size of the prediction errors, without considering whether the errors are positive or negative. *MAE* provides a simple and intuitive understanding of model performance by treating all errors equally, making it an effective metric for understanding the typical prediction error across the dataset (Sun and Ling, 2022). The mathematical expression for *MAE* is given as:

$$MAE = \frac{1}{n}\sum_{i=1}^{n}|y_i - \hat{y}_i| \quad (14)$$

The coefficient of determination, denoted as R^2, serves as an essential metric for evaluating the proportion of variance in the target variable that is explained by the model's input features (Andorra *et al*., 2018). R^2 values range from 0-1, with a value closer to 1 signifying that the model achieves a higher level of predictive accuracy. In essence, a higher R^2 indicates a better fit of the model to the actual data. The formula for calculating R^2 is as follows:

$$R^2 = 1 - \frac{\sum_{i=1}^{n}(y_i - \hat{y}_i)^2}{\sum_{i=1}^{n}(y_i - \bar{y})^2} \quad (15)$$

Activation Function Evaluation

The activation function evaluation of the MLP-ANN prediction model's performance was carried out using four key metrics: Percentage of dead neurons, smoothness score, and final training loss.

Percentage of Dead Neurons

The percentage of potential dead neurons is a critical metric that highlights the proportion of neurons in a network that becomes inactive during training. A neuron is considered "dead" if it consistently outputs zero for any given input, thus contributing nothing to the learning process (Jo *et al*., 2020). To measure the percentage of dead neurons, one can monitor the activations of each neuron over multiple training epochs. The metric is calculated as follows:

$$P_{dead} = \frac{\sum_{i=1}^{N} 1(a_i = 0)}{N} \times 100 \quad (16)$$

where, $1(a_i = 0)$ is an indicator function that equals 1 if the activation a_i of neuron i is zero and N is the total number of neurons. A high percentage of dead neurons suggests a need for alternative activation functions or modifications such as leaky ReLU or parametric ReLU (PReLU), which can help maintain non-zero gradients and ensure more neurons remain active.

The Smoothness Score

The smoothness score of an activation function measures the degree to which the function produces continuous and differentiable outputs (Kılıçarslan *et al*., 2021). Smoothness can be quantitatively assessed through the second derivative of the activation function or by evaluating the variance of the gradients during training. Mathematically, the smoothness score S can be approximated by:

$$S = \frac{1}{N}\sum_{i=1}^{N}\left|\frac{\vartheta^2 f(x_i)}{\vartheta x^2}\right| \quad (17)$$

where, $f(x_i)$ represents the activation function applied to input x_i and N is the number of inputs. Lower values of S indicate a smoother function. For empirical evaluation, the variance of the gradients can be monitored:

$$Var(\nabla W) = \frac{1}{N}\sum_{i=1}^{N}(\nabla W_i - \overline{\nabla W})^2 \quad (18)$$

where, ∇W_i is the gradient of weight i and ∇W is the mean gradient. A high variance may indicate sharp changes introduced by the activation function, potentially disrupting the learning process.

Final Training Loss

Final training loss is a direct indicator of how well the neural network has learned from the training data (Javid *et al*., 2021). It reflects the discrepancy between the network's predictions and the actual data, with lower values indicating better performance. Training loss L can be computed using various loss functions, depending on the nature of the task. For regression tasks, the Mean Squared Error (MSE) is commonly used:

$$L_{MSE} = \frac{1}{N}\sum_{i=1}^{N}(y_i - \hat{y}_i)^2 \quad (19)$$

where, y_i is the actual value, $\hat{y}_i$ is the predicted value and N is the number of samples.

Results

The experiment utilized several powerful tools and libraries within the Python programming environment to develop and evaluate the models. Key libraries employed included keras-tuner, TensorFlow, matplotlib, NumPy, pandas, scikit-learn, and time. These tools provided a comprehensive framework for constructing, optimizing, and assessing machine learning models. The data collection took place across three distinct regions Zone 1-3 at four different time intervals: 5, 15, 30, and 60 min. The datasets for the 15, 30, and 60 min intervals were generated by aggregating and calculating multiples of the base 5-min dataset. Specifically, for each longer interval, the features were calculated as the sum or average (where applicable) of the corresponding data points from the base 5-min intervals, ensuring a representative summary of the conditions over the longer time spans. The number of

occupants, their activities, and the use of electronic devices were manually recorded through CCTV camera observations. Over the 14-week period, a total of 478 individuals were present in the observed zones, representing 85.35% of the overall population of 560 in the area. Table (6) presents a detailed summary of the dataset, including total records and the number of records for each zone.

Proper Time Interval of Dataset

The performance of these polynomial models was evaluated by calculating the R-squared value for each day in each zone, providing a measure of how well the models fit the observed data. Tables (7-10) present the R-squared values for the polynomial regression analysis of 2nd degree (quadratic) applied to the cooling load data collected at various time intervals (5, 15, 30, and 60 min) across three zones (Zone 1-3) from Monday-Friday.

The proper dataset-based high R-squared comprises selecting the 30-min interval for Thursday in Zone 2, alongside other days' preferred intervals. Specifically, Zone 1 shows the highest R-squared values with the 60-min interval for all days except Thursday, where the 30-min interval is optimal. Similarly, Zone 2 prefers the 30-min interval for Monday and Tuesday, the 60-min interval for Wednesday and Friday, and the 30-min interval for Thursday. Zone 3 consistently favors the 60-min interval across all days of the week. The selected time interval is shown in Table (11).

Table 6: Dataset description

Dataset	Total records	Number of records		
		Zone 1	Zone 2	Zone 3
5 min	15,022	5,095	4,918	5,009
15 min	5,103	1,738	1,682	1,683
30 min	2,639	898	870	871
60 min	1,407	478	464	465

Table 7: Polynomial regression 2nd degree of 5 min dataset

Zone	R-squared				
	M	T	W	TH	F
1	0,0266	0,0486	0,0524	0,0331	0,0323
2	0,0444	0,0326	0,0458	0,0047	0,0091
3	0,0294	0,0122	0,0055	0,0021	0,0228

Table 8: Polynomial regression 2nd degree of 15 min dataset

Zone	R-squared				
	M	T	W	TH	F
1	0,0469	0,0688	0,0714	0,0448	0,0502
2	0,0563	0,0380	0,0672	0,0067	0,0139
3	0,0441	0,0176	0,0078	0,0027	0,0642

Table 9: Polynomial regression 2nd degree of 30 min dataset

Zone	R-squared				
	M	T	W	TH	F
1	0,0559	0,0855	0,0770	0,0490	0,0635
2	0,0589	0,0418	0,0732	0,0085	0,0170
3	0,0519	0,0206	0,0094	0,0034	0,0772

Table 10: Polynomial regression 2nd degree of 60 min dataset

Zone	R-squared				
	M	T	W	TH	F
1	0,0737	0,093	0,0809	0,0482	0,0675
2	0,0576	0,0414	0,0763	0,0085	0,0182
3	0,0566	0,0225	0,0097	0,0035	0,0782

Table 11: Proper time interval of the dataset

Zone	Time interval				
	M	T	W	TH	F
1	60 min	60 min	60 min	30 min	60 min
2	30 min	30 min	60 min	30 min	60 min
3	60 min	60 min	60 min	60 min	60 min

Table 12: Low-variance variables (variance <0.1)

Variable	Variance score	Status
Num-sleep	0,011397	Not valid
Num-typing	0,001145	Not valid
Indoor-air-pressure	0,000311	Not valid
Outdoor-air-pressure	0,000245	Not valid

Dataset Validity and Reliability

The examination of variance in the dataset, as outlined in Table (12) revealed clear distinctions between low and high-variance features. The low-variance variables included num-sleep, num-typing, indoor-air-pressure, and outdoor-air-pressure, all exhibiting variance scores of less than 0.1. As a result, these variables were marked as "Not Valid" due to their limited influence on the dataset's dynamics.

The Exploratory Factor Analysis (EFA) performed on the dataset, as illustrated in Fig. (13), sought to identify the optimal number of factors that best capture the underlying structure of the data. The scree plot, depicted in Fig. (2), displays the eigenvalues corresponding to each factor, revealing a notable "elbow" point at the fourth factor. This elbow indicates that the first four factors account for the most substantial variance within the dataset, making them the most influential in explaining the data's structure. Beyond this point, additional factors contribute only marginally to the explanation of variance. This suggests that the first four factors are sufficient to represent the essential patterns and relationships in the data, with diminishing returns from including further factors in the analysis.

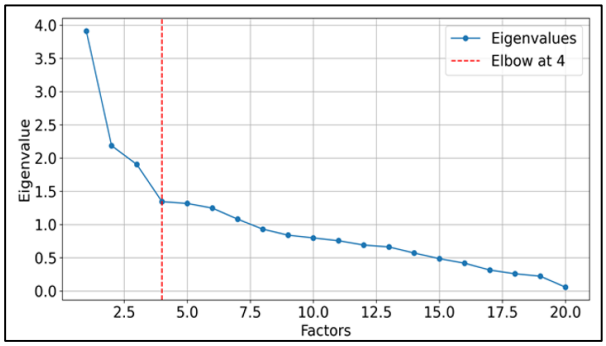

Fig. 2: The scree plot dataset

The factor loadings heatmap in Fig. (3) provides a comprehensive visualization of how different variables relate to the extracted factors in the dataset. The heatmap uses color intensity to represent the magnitude of the loadings, with red indicating positive loadings and blue indicating negative loadings.

In the first category, which includes occupant behavior variables such as num-light-work, num-walk, num-write, num-stand, num-read, num-talk, num-occupant, and num-squat, high loadings are observed on factor 1. This suggests that factor 1 is primarily associated with the variability in how occupants utilize the space and engage in various activities. The second category focuses on electronic usage variables, specifically num-mobile phone, and num-computer, which show significant loadings on factor 2. This factor highlights the critical role of technology in the environment, as electronic devices generate heat that must be managed by the cooling system. Environmental conditions variables, such as outdoor-hum and indoor-hum, are included in the third category and show high loadings on Factors 3 and 4, respectively. The refined correlation matrix displayed in Fig. (4) illustrates the interrelationships among the selected features after addressing issues related to low-variance and the insights derived from the factor loadings heatmap.

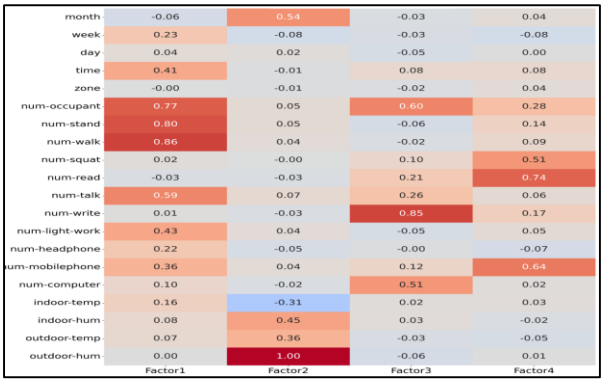

Fig. 3: Factor loadings heatmap

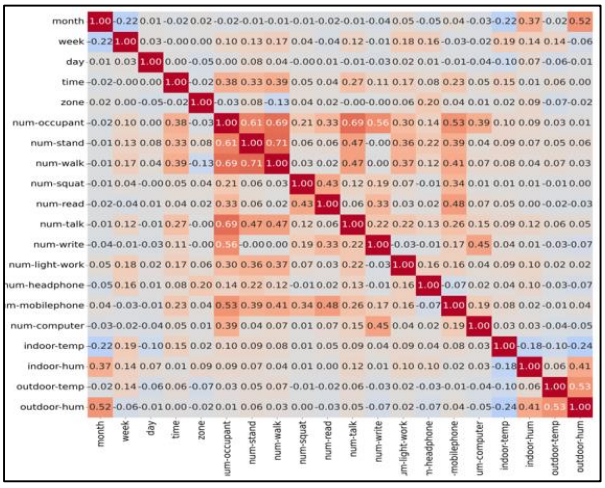

Fig. 4: Correlation matrix of selected features

The correlation matrix reveals strong positive correlations among several occupant behavior variables. The dataset was refined by eliminating redundant and low-variance features based on the analysis of highly correlated pairs (correlation >0.8 or <-0.8) and the factor loadings heatmap. The resulting set of selected features included occupant behavior variables: Num-light-work, num-walk, num-write, num-stand, num-read, num-talk, num-occupant, and num-squat; electronic usage variables: Num-mobile phone and num-computer and environmental conditions variables: Outdoor-hum and indoor-hum.

Cooling Load-Based MLP-ANN

The development of the cooling load model in this study leverages a Multi-Layer Perceptron-Artificial Neural Network (MLP-ANN) and focuses on the original dataset which consists of selected features and incorporation of feature engineering. The experimental setup includes two main configurations: The baseline model and the proposed model.

Baseline Model

The hyperparameter tuning results, as detailed in Table (13), reveal significant insights into the optimal configurations for the MLP-ANN models using ReLU, PReLU, and leaky ReLU activation functions. Each model was fine-tuned to achieve the best performance, reflecting the nuanced adjustments necessary for optimizing neural network architectures.

The regression analysis of the hyperparameter-tuned baseline MLP-ANN models, as depicted in Figs. (5-7), provides a rigorous examination of the relationship between predicted and actual values using different standard activation functions ReLU, PReLU, and leaky ReLU.

Table 13: Result of hyperparameter-tuned baseline model

Parameter	1st model	2nd model	3rd model
Neuron in 1st hidden layer	96	96	128
Dropout rate in 1st hidden layer	0.2	0.1	0.2
Learning rate	0.00930	0.00860	0.00777
Activation function	ReLU	PReLU	Leaky ReLU

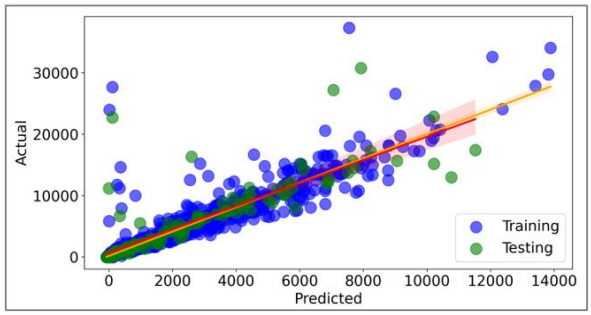

Fig. 5: Baseline model with ReLU

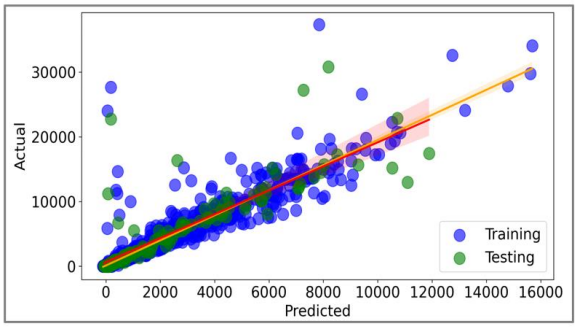

Fig. 6: Baseline model with PreLU

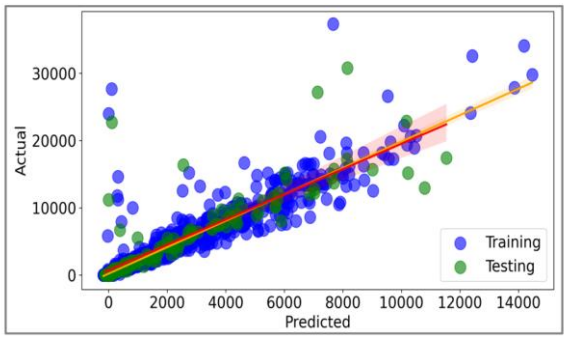

Fig. 7: Baseline model with leaky ReLU

In Fig. (5), the regression plot for the ReLU activation function displays a strong correlation between predicted and actual values, particularly in the lower to mid-range. The regression line follows the diagonal closely, indicating effective data trend capture. Figure (6) shows the PReLU activation function with a similarly strong correlation across the full data range. The well-aligned regression line and narrower spread in testing data, compared to ReLU, suggest that PReLU's adaptive slope and hyperparameter tuning enhance performance, though minor errors appear in higher values. In Fig. (7), the leaky ReLU function shows a comparable pattern, with robust alignment between predicted and actual values. Hyperparameter tuning minimizes deviations, reducing residual spread.

Proposed Model

The results of hyperparameter tuning for the proposed model, as detailed in Table (14), provide valuable insights into the optimal configurations for MLP-ANN models with different weight scales. The investigation covered four different scales (0.5, 1.0, 1.5, and 2.0) using custom GlorotUniform weight initialization, allowing for a comprehensive analysis of how varying scales impact model performance. Table (14) details the hyperparameters tuned for the proposed models, revealing three distinct configurations.

The regression analysis of the proposed MLP-ANN models, as depicted in Figs. (8-10), provides a comprehensive examination of the relationship between actual and predicted values across different configurations of custom activation functions with bias ReLU with bias, PReLU with bias, and leaky ReLU with bias. The dataset used for this analysis was feature-engineered, with weight initialization performed using the GlorotUniform method, scaled according to the specific configurations: ReLU with bias and a custom weight scale of 2.0, PReLU with bias and a custom weight scale of 1.0 and leaky ReLU with bias and a custom weight scale of 2.0.

Table 14: Result of hyperparameter-tuned proposed model

Parameter	1st model	2nd model	3rd model
Neuron in 1st hidden layer	96	96	128
Dropout rate in 1st hidden layer	0.1	0.1	0.3
Learning rate	0.00979	0.00641	0.00602
Scale of custom Glorot uniform Weight initialization	2.0	1.0	2.0
Activation function	ReLU with bias	PreLU with bias	Leaky ReLU with bias

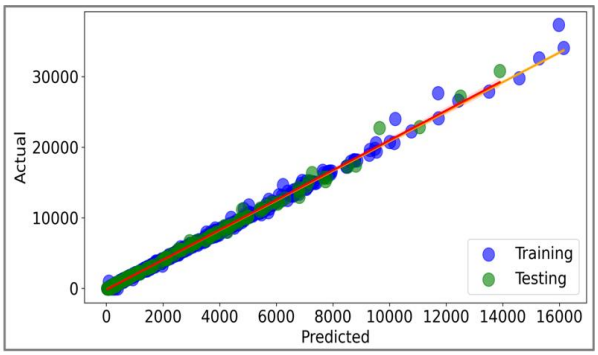

Fig. 8: Proposed model-ReLU with bias and custom weight scale 2.0

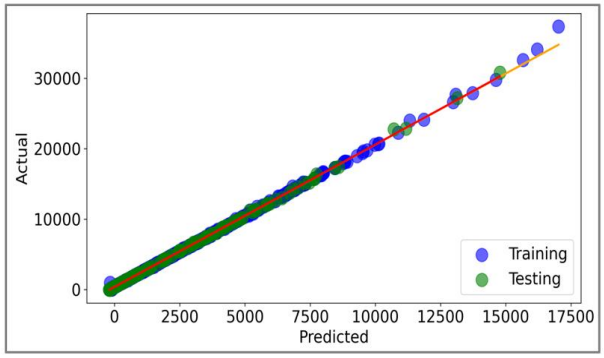

Fig. 9: Proposed model-PReLU with bias and custom weight scale 1.0

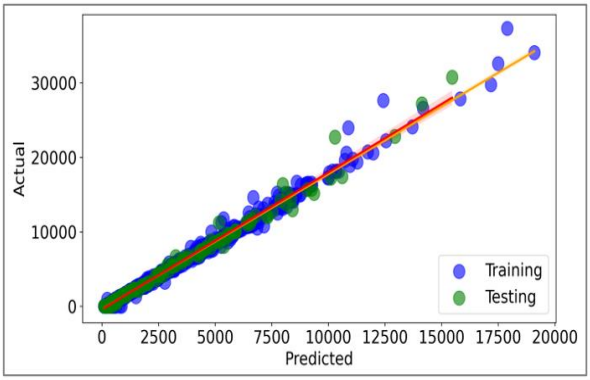

Fig. 10: Proposed model-leaky ReLU with bias and custom weight scale 2.0

In Fig. (8), the regression plot for ReLU with bias and a custom weight scale of 2.0 shows a strong linear relationship between predicted and actual values, particularly in the mid to upper range. The regression line closely follows the diagonal, indicating that the model captures the data trend effectively. Figure (9) shows the PReLU with bias and a custom weight scale of 1.0, which also demonstrates a strong correlation across the full range of values. The tight alignment of the regression line suggests effective generalization, with a narrower spread of points indicating improved predictive accuracy, especially in handling data variations. In Fig. (10), the leaky ReLU with bias and a custom weight scale of 2.0 displays the strongest alignment, with minimal spread around the regression line, reflecting the model's high accuracy in capturing data variability across all ranges.

Model Performance

The evaluation of the proposed model performance, as detailed in Tables (15-16), involves assessing the key metrics of Root Mean Squared Error (RMSE), Mean Absolute Error (MAE), and the coefficient of determination (R^2) for baseline and proposed model.

Table 15: Performance of baseline model

Activation function	RMSE	MAE	R^2
ReLU	1919.2059	938.7655	0.8105
PReLU	1906.3475	942.2942	0.8141
Leaky ReLU	1913.9209	937.3667	0.8123

Table 16: Performance of the proposed model

Activation function	RMSE	MAE	R^2
ReLU with bias and scale of weight 2.0	144.1488	84.8169	0.9990
PReLU with bias and scale of weight 1.0	174.0528	100.5422	0.9986
Leaky ReLU with bias and scale of weight 2.0	128.2615	90.6529	0.9992

The baseline models using standard ReLU, PReLU, and leaky ReLU activation functions exhibit moderate performance, with RMSE values ranging from 1906-1919, MAE values around 937-942, and R^2 scores between 0.8105 and 0.8141. This suggests that while these models capture much of the variance, their predictions contain significant errors.

In contrast, the proposed models incorporating bias and custom weight scaling demonstrate substantially improved performance. The ReLU with a bias and weight scale of 2.0 achieved an RMSE of 144.1488, an MAE of 84.8169, and an R^2 of 0.9990, indicating near-perfect prediction accuracy. Similarly, PReLU with bias and a weight scale of 1.0 and leaky ReLU with bias and a weight scale of 2.0, produced RMSE values of 174.0528 and 128.2615, respectively, and R^2 scores exceeding 0.9986, showcasing their ability to significantly reduce prediction errors and accurately model the data.

This evaluation underscores the superior effectiveness of the proposed model configurations, highlighting the transformative role of incorporating bias and custom weight scaling in enhancing predictive precision across all metrics. The remarkable reduction in RMSE and MAE, coupled with near-perfect R^2 values, demonstrates the models' capacity to generalize effectively across both training and testing datasets, far surpassing the performance of baseline models.

Activation Function Performance

The evaluation of activation function performance for both baseline and proposed models reveals significant differences in key metrics, offering a nuanced understanding of model behavior. Table (17) demonstrates that the baseline models utilizing ReLU, PReLU, and leaky ReLU activation functions exhibit no dead neurons, with smoothness scores ranging from 0.42-0.61. However, their high final training losses, exceeding 5.7 million, indicate potential limitations in capturing finer details within the data.

Table 17: Activation function performance of baseline model

Activation function	Dead neurons (%)	Smoothness (min, max)	Final loss
ReLU	0	[0.42, 3436.10]	5,716,996
PReLU	0	[0.61, 3454.89]	5,761,277
Leaky ReLU	0	[0.47, 3453.39]	5,768,892

Table 18: Activation function performance of the proposed model

Activation function	Dead neurons (%)	Smoothness (min, max)	Final loss
ReLU with bias and scale of weight 2.0	0.83	(1.24, 4180.92)	1,034,874
PReLU with bias and scale of weight 1.0	0	(0.84, 4119.27)	1,354,475
Leaky ReLU with bias and scale of weight 2.0	0	(0.86, 4139.38)	1,328,669

Table 19: Comparison with state-of-the-art

Model	RMSE	MAE	R^2
Hyperparameter-tuned of proposed MLP-ANN	128.2615	90.6529	0.9992
proposed MLP-ANN	937.4965	617.4522	0.9089
Support Vector Regression (SVR)	1883.0656	682.7518	0.8628
Elastic-Net (ELN)	1343.5978	568.8377	0.9301
Extreme Gradient Boosting (XGB)	1213.1228	610.6796	0.9430
Long Short-Term Memory (LSTM)	1409.2593	704.0370	0.9231
Recurrent Neural Network (RNN)	1469.7885	963.8216	0.9164

In contrast, the proposed models in Table (18), which integrate bias and custom weight scaling, show more refined performance. The ReLU with bias and a weight scale of 2.0 exhibits a small percentage of dead neurons (0.83%) but significantly reduces the final training loss to 1,034,874.613. PReLU with bias and a scale of 1.0 and leaky ReLU with bias and a scale of 2.0 both maintain 0% dead neurons, demonstrating their resilience. Notably, these models achieve much lower final losses compared to the baseline, with PReLU at 1,354,475 and leaky ReLU at 1,328,669. The increased smoothness scores in the proposed models reflect their improved capacity for generalization, with smoother transitions in neuron activation contributing to more stable and accurate predictions. This analysis underscores the enhanced efficacy of bias integration and custom weight scaling, offering considerable improvements in model performance over the baseline activation functions.

State-of-the-Art Comparison

Table (19) describes the comparative analysis of the proposed MLP-ANN model (Leaky ReLU with bias and scale of weight 2.0) with state-of-the-art machine learning methods, including Support Vector Regression (SVR) (Moradzadeh *et al*., 2022), E-Lastic-Net (ELN) (Sha *et al*., 2021), Extreme Gradient Boosting (XGB) (Fan *et al*., 2017), Long Short-Term Memory (LSTM) (Chaganti *et al*., 2022) and Recurrent Neural Network (RNN) (Sha *et al*., 2021), reveals significant insights into the effectiveness of different modeling approaches.

The hyperparameter-tuned MLP-ANN model outperforms all other methods, achieving an RMSE of 128.2615, an MAE of 90.6529, and an R^2 of 0.9992, indicating near-perfect prediction accuracy and minimal error. In contrast, the baseline MLP-ANN model, while still competitive with an R^2 of 0.9089, exhibits higher error metrics compared to its tuned counterpart. Among the other models, XGB demonstrates strong performance with an RMSE of 1213.1228 and an R^2 of 0.9430, closely followed by ELN and LSTM. However, methods like SVR and RNN fall behind, with higher RMSE and MAE values, signaling weaker predictive power. This comparison underscores the superiority of the proposed hyperparameter-tuned MLP-ANN model, highlighting its enhanced ability to generalize and deliver accurate predictions across varying conditions.

Discussion

The discussion of the experimental results highlights the significant improvements achieved by the proposed MLP-ANN models over both the baseline models and other state-of-the-art machine learning methods. By incorporating bias and custom weight scaling into the activation functions, the proposed models demonstrated enhanced predictive performance, evidenced by substantially reduced Root Mean Squared Error (RMSE), Mean Absolute Error (MAE) values, and nearly perfect R^2 scores. These findings underline the critical role of hyperparameter tuning in optimizing neural network performance for complex tasks, such as cooling load prediction.

The results of this study indicate that the hyperparameter-tuned MLP-ANN model with custom GlorotUniform weight initialization and bias significantly outperforms traditional models, such as Support Vector Regression (SVR), E-Lastic-Net (ELN), and Recurrent Neural Networks (RNN). For instance, the RMSE of the proposed model using Leaky ReLU with bias and a weight scale of 2.0 was 128.26, while SVR and ELN achieved RMSE values of 1883.07 and 1343.60, respectively, in prior studies (Guo *et al*., 2023; Sha *et al*., 2021). These results highlight the limitations of traditional statistical and kernel-based methods in capturing the nonlinearities and temporal dependencies inherent in under-actuated zone cooling loads.

Compared to advanced machine learning techniques such as Extreme Gradient Boosting (XGB) and Long Short-Term Memory (LSTM), the proposed model also demonstrated superior performance. XGB and LSTM models reported RMSE values of 1213.12 and 1409.26, respectively (Fan *et al*., 2017; Chaganti *et al*., 2022), while the proposed MLP-ANN model achieved a significantly lower RMSE. This reduction can be attributed to the introduction of trainable bias in activation functions and the custom Glorot weight scaling, which enhanced the model's ability to adapt to complex, multi-factorial data.

The adaptive power of advanced activation functions, such as PReLU and Leaky ReLU with bias, is particularly evident in their capacity to handle the nonlinearities and variations within the dataset. Unlike traditional activation functions such as standard ReLU, which are prone to the "dying ReLU" problem (Kulathunga *et al*., 2021), the proposed activation functions effectively maintained gradient flow, as evidenced by a low percentage of dead neurons (0% for Leaky ReLU with bias).

The regression analysis demonstrated minimal deviations from the regression line for the proposed

models, indicating their robustness in accurately modeling complex relationships between occupant behavior, environmental factors, and electronic device usage. Similar results were observed in the study by Moradzadeh *et al*. (2022), which highlighted the importance of feature interactions in enhancing predictive performance; however, the present study's integration of trainable bias further improved adaptability and generalization.

The findings are further supported by Exploratory Factor Analysis (EFA) and feature selection, which identified critical factors influencing cooling load predictions. The scree plot and factor loadings heatmap demonstrated that occupant behavior (e.g., num-walk, num-talk) and electronic usage (e.g., num-computer, num-mobile phone) were the most significant contributors to cooling load variability. This aligns with prior studies, such as Yang *et al*. (2022), which emphasized the importance of occupant-centric features in HVAC optimization. However, unlike previous works that relied on static or oversimplified models, this study's feature engineering process, including sine-cosine transformations and lag features, enabled the MLP-ANN to better capture temporal and cyclical patterns, further improving predictive accuracy. Additionally, the removal of low-variance features (e.g., num-sleep, indoor-air-pressure) enhanced the model's efficiency by focusing on the most relevant and dynamic variables, an approach that parallels methodologies adopted by Zhang *et al*. (2020).

From a practical perspective, the proposed models' superior performance metrics, including a 32.6% reduction in RMSE compared to state-of-the-art methods like XGB, demonstrate their potential for real-world implementation in HVAC systems for under-actuated zones. These advancements not only improve energy efficiency but also ensure enhanced occupant comfort by accurately predicting cooling loads in dynamic and variable environments.

Conclusion

The experimental work presented in this study offers several significant conclusions, both in terms of its scientific contribution and its broader economic implications. First, the introduction of bias and custom weight scaling in the activation functions of the MLP-ANN model has been shown to substantially enhance predictive performance. By carefully tuning hyperparameters and leveraging advanced activation functions such as PReLU and leaky ReLU with bias, the proposed models demonstrated remarkable improvements in accuracy, as evidenced by lower RMSE and MAE values, along with nearly perfect R^2 scores. This finding underscores the importance of incorporating adaptive mechanisms within neural network architectures to optimize their ability to model complex, nonlinear systems such as cooling load predictions in under-actuated zones.

The comparative analysis with state-of-the-art machine learning methods such as Support Vector Regression, E-Lastic-Net, and Recurrent Neural Networks revealed the clear superiority of the proposed MLP-ANN model. This superiority is particularly evident in the model's capacity to generalize across both training and testing datasets, indicating its robustness and versatility. This advancement contributes meaningfully to the field of machine learning by showcasing the potential of advanced neural network configurations in tackling real-world predictive tasks with high degrees of variability and complexity.

From an economic perspective, the ability to accurately predict cooling loads in under-actuated zones has profound implications for energy management systems, particularly in the optimization of HVAC systems. Enhanced prediction accuracy directly translates into more efficient energy usage, minimizing unnecessary cooling while ensuring occupant comfort. This leads to substantial energy savings and reduced operational costs, offering significant economic benefits for building managers and facility operators. Moreover, the implementation of such predictive models could support the development of smart buildings, contributing to broader sustainability goals by optimizing resource consumption and reducing carbon footprints.

The contribution of this study to the scientific community lies not only in the proposed model's enhanced performance but also in its methodological rigor. The systematic refinement of the dataset, including the elimination of low-variance and redundant features, provided a clear pathway for future research to adopt similar strategies in predictive modeling. Furthermore, the integration of occupant behavior, environmental conditions, and electronic usage into the model serves as a foundational step towards more comprehensive, occupant-centric approaches in the design of energy-efficient systems.

In conclusion, this study bridges the gap between advanced machine learning techniques and practical applications in energy management. The findings provide a solid foundation for further exploration of real-time predictive control in HVAC systems and establish a precedent for future research focused on optimizing energy efficiency in smart buildings, contributing to both scientific advancement and economic sustainability.

Acknowledgment

We would like to express our sincere gratitude to all those who contributed to the successful completion of this research. First and foremost, we extend our heartfelt appreciation to our supervisors at Asia e University (A e U) and Universiti Kuala Lumpur (Uni KL), Prof. Aedah Binti Abd Rahman, and Ts. Dr. Amna Saad, for their

invaluable guidance, encouragement, and insightful feedback throughout the project. We would also like to thank Universitas Trilogi for giving permission to use the library as the object of research.

Funding Information

We are indebted to the Department of Higher Education, Ministry of Education and Culture of Indonesia for providing funding to conduct this research, without which this study would not have been possible.

Author's Contributions

Yaddarabullah: Designed and conceptualized the study, coordinated research activities, collected and analyzed data, conducted the literature review, interpreted the results, and prepared the manuscript.

Aedah Abd Rahman: Contributed to data interpretation, critically reviewed the manuscript, and provided key insights for the discussion.

Amna Saad: Guided model performance and statistical analysis, interpreted data, and critically reviewed the manuscript, offering important input for the discussion section.

Ethics

This research study was conducted in accordance with the ethical principles outlined by the Department of Higher Education, Ministry of Education and Culture of Indonesia, and in compliance with relevant international regulations. The authors declare that there is no conflict of interest that could have influenced the conduct or reporting of this research. The data from this study can be obtained by contacting the corresponding author directly via email.

References

Ahmed, O., Sezer, N., Ouf, M., Wang, L. (Leon), & Hassan, I. G. (2023). State-of-the-Art Review of Occupant Behavior Modeling and Implementation in Building Performance Simulation. *Renewable and Sustainable Energy Reviews*, *185*, 113558. https://doi.org/10.1016/j.rser.2023.113558

Andorra, M., Nakamura, K., Lampert, E. J., Pulido-Valdeolivas, I., Zubizarreta, I., Llufriu, S., Martinez-Heras, E., Sola-Valls, N., Sepulveda, M., Tercero-Uribe, A., Blanco, Y., Saiz, A., Villoslada, P., & Martinez-Lapiscina, E. H. (2018). Assessing Biological and Methodological Aspects of Brain Volume Loss in Multiple Sclerosis. *JAMA Neurology*, *75*(10), 1246–1255. https://doi.org/10.1001/jamaneurol.2018.1596

Al-Shargabi, A. A., Almhafdy, A., Ibrahim, D. M., Alghieth, M., & Chiclana, F. (2021). Tuning Deep Neural Networks for Predicting Energy Consumption in Arid Climate Based on Buildings Characteristics. *Sustainability*, *13*(22), 12442. https://doi.org/10.3390/su132212442

Bathia, A. (2014). *HVAC Cooling Load - Calculations and Principles: Quick Book*.

Brooks, J., Kumar, S., Goyal, S., Subramany, R., & Barooah, P. (2015). Energy-Efficient Control of Under-Actuated HVAC Zones in Commercial Buildings. *Energy and Buildings*, *93*, 160–168. https://doi.org/10.1016/j.enbuild.2015.01.050

Chaganti, R., Rustam, F., Daghriri, T., Díez, I. de la T., Mazón, J. L. V., Rodríguez, C. L., & Ashraf, I. (2022). Building Heating and Cooling Load Prediction Using Ensemble Machine Learning Model. *Sensors*, *22*(19), 7692. https://doi.org/10.3390/s22197692

Fan, C., Xiao, F., & Zhao, Y. (2017). A Short-Term Building Cooling Load Prediction Method Using Deep Learning Algorithms. *Applied Energy*, *195*, 222–233. https://doi.org/10.1016/j.apenergy.2017.03.064

Gao, Y., Hang, Y., & Yang, M. (2021). A Cooling Load Prediction Method Using Improved CEEMDAN and Markov Chains Correction. *Journal of Building Engineering*, *42*, 103041. https://doi.org/10.1016/j.jobe.2021.103041

Ghaffari Jabbari, S., Maleki, A., Kaynezhad, M. A., & Olesen, B. W. (2020). Inter-Personal Factors Affecting Building Occupants' Thermal Tolerance at Cold Outdoor Condition During an Autumn–Winter Period. *Indoor and Built Environment*, *29*(7), 987–1005. https://doi.org/10.1177/1420326x19867999

Guo, J., Yun, S., Meng, Y., He, N., Ye, D., Zhao, Z., Jia, L., & Yang, L. (2023). Prediction of Heating and Cooling Loads Based on Light Gradient Boosting Machine Algorithms. *Building and Environment*, *236*, 110252. https://doi.org/10.1016/j.buildenv.2023.110252

Hashim, H. M., Sokolova, E., Derevianko, O., & Solovev, D. B. (2018). Cooling Load Calculations. *IOP Conference Series: Materials Science and Engineering*, *463*(3), 032030. https://doi.org/10.1088/1757-899x/463/3/032030

Hussein, M. M. F., Saeed, A. A., & Husen, M. S. (2023). Comparison Markov Chain and Neural Network Models for Forecasting Population Growth Data in Iraq. *University of Kirkuk Journal for Administrative and Economic Science*, *13*(4), 1–14.

Japa, L., Serqueira, M., MendonçA, I., Aritsugi, M., Bezerra, E., & González, P. H. (2023). A Population-Based Hybrid Approach for Hyperparameter Optimization of Neural Networks. *IEEE Access*, *11*, 50752–50768. https://doi.org/10.1109/access.2023.3277310

Javid, A. M., Das, S., Skoglund, M., & Chatterjee, S. (2021). A ReLU Dense Layer to Improve the Performance of Neural Networks. *ICASSP 2021-2021 IEEE International Conference on Acoustics, Speech and Signal Processing (ICASSP)*, 2810–2814. https://doi.org/10.1109/icassp39728.2021.9414269

Jo, Y. S., Namboodiri, V. M. K., Stuber, G. D., & Zweifel, L. S. (2020). Persistent Activation of Central Amygdala CRF Neurons Helps Drive the Immediate Fear Extinction Deficit. *Nature Communications*, *11*(1), 422. https://doi.org/10.1038/s41467-020-14393-y

Kamińska, J. A., Sciavicco, G., Lucena-Sánchez, E., & Jiménez, F. (2020). Lag Variables in Air Pollution Modeling Based on Traffic Flow and Meteorological Factors. *Proceedings*, *51*(1), 1. https://doi.org/10.3390/proceedings2020051001

Kılıçarslan, S., Adem, K., & Çelik, M. (2021). An Overview of the Activation Functions Used in Deep Learning Algorithms. *Journal of New Results in Science*, *10*(3), 75–88. https://doi.org/10.54187/jnrs.1011739

Kim, H.-J., & Cho, Y.-H. (2022). Optimization of Supply Air Flow and Temperature for VAV Terminal Unit by Artificial Neural Network. *Case Studies in Thermal Engineering*, *40*, 102511. https://doi.org/10.1016/j.csite.2022.102511

Kim, H.-J., Shin, J.-H., Jo, J. H., & Cho, Y.-H. (2020). Development of Air Flow Rate Prediction Model Using Multiple Regression in VAV Terminal Unit. *Energies*, *13*(10), 2667. https://doi.org/10.3390/en13102667

Kim, S., & McMahon, D. G. (2021). Light Sets the Brain's Daily Clock by Regional Quickening and Slowing of the Molecular Clockworks at Dawn and Dusk. *BioRxiv*, *10*, 1–31. https://doi.org/10.1101/2020.06.05.136440

Kong, M., Dong, B., Zhang, R., & O'Neill, Z. (2022). HVAC Energy Savings, Thermal Comfort and Air Quality for Occupant-Centric Control Through a Side-by-Side Experimental Study. *Applied Energy*, *306*, 117987. https://doi.org/10.1016/j.apenergy.2021.117987

Kuiper, R. M., & Ryan, O. (2018). Drawing Conclusions from Cross-Lagged Relationships: Re-Considering the Role of the Time-Interval. *Structural Equation Modeling: A Multidisciplinary Journal*, *25*(5), 809–823. https://doi.org/10.1080/10705511.2018.1431046

Kulathunga, N., Ranasinghe, N. R., Vrinceanu, D., Kinsman, Z., Huang, L., & Wang, Y. (2021). Effects of Nonlinearity and Network Architecture on the Performance of Supervised Neural Networks. *Algorithms*, *14*(2), 51. https://doi.org/10.3390/a14020051

Lee, J., Yim, M. H., & Kim, J. Y. (2018). Test-Retest Reliability of the Questionnaire in the Sasang Constitutional Analysis Tool (SCAT). *Integrative Medicine Research*, *7*(2), 136–140. https://doi.org/10.1016/j.imr.2018.02.001

Li, H., Shang, L., Li, C., & Lei, J. (2023). Research on Air-Conditioning Cooling Load Correction and Its Application Based on Clustering and LSTM Algorithm. *Applied Sciences*, *13*(8), 5151. https://doi.org/10.3390/app13085151

Li, X., & Yao, R. (2020). A Machine-Learning-Based Approach to Predict Residential Annual Space Heating and Cooling Loads Considering Occupant Behaviour. *Energy*, *212*, 118676. https://doi.org/10.1016/j.energy.2020.118676

Moradzadeh, A., Mohammadi-Ivatloo, B., Abapour, M., Anvari-Moghaddam, A., & Roy, S. S. (2022). Heating and Cooling Loads Forecasting for Residential Buildings Based on Hybrid Machine Learning Applications: A Comprehensive Review and Comparative Analysis. *IEEE Access*, *10*, 2196–2215. https://doi.org/10.1109/access.2021.3136091

Olimov, B., Karshiev, S., Jang, E., Din, S., Paul, A., & Kim, J. (2021). Weight Initialization Based-Rectified Linear Unit Activation Function to Improve the Performance of a Convolutional Neural Network Model. *Concurrency and Computation: Practice and Experience*, *33*(22), e6143. https://doi.org/10.1002/cpe.6143

Ruddell, B. L., Salamanca, F., & Mahalov, A. (2014). Reducing a Semiarid City's Peak Electrical Demand Using Distributed Cold Thermal Energy Storage. *Applied Energy*, *134*, 35–44. https://doi.org/10.1016/j.apenergy.2014.07.096

Sagar, P., Gupta, P., & Kashyap, I. (2021). A Forecasting Method with Efficient Selection of Variables in Multivariate Data Sets. *International Journal of Information Technology*, *13*(3), 1039–1046. https://doi.org/10.1007/s41870-021-00619-9

Sha, H., Moujahed, M., & Qi, D. (2021). Machine Learning-Based Cooling Load Prediction and Optimal Control for Mechanical Ventilative Cooling in High-Rise Buildings. *Energy and Buildings*, *242*, 110980. https://doi.org/10.1016/j.enbuild.2021.110980

Sholahudin, S., & Han, H. (2016). Simplified Dynamic Neural Network Model to Predict Heating Load of a Building Using Taguchi Method. *Energy*, *115*, 1672–1678. https://doi.org/10.1016/j.energy.2016.03.057

Sultana, S., Athientis, A. K., & Zmeureanu, R. G. (2019). Improving Energy Savings of a Library Building through Mixed Mode Hybrid Ventilation. *Symposium on Energy Efficiency in Buildings and Industry*, *23*(1), 3. https://doi.org/10.3390/proceedings2019023003

Sun, T., & Ling, F. (2022). Prediction Method of Wheat Moisture Content in the Hot Air Drying Process Based on Backpropagation Neural Network Optimized by Genetic Algorithms. *Journal of Food Processing and Preservation*, *46*(6), e16565. https://doi.org/10.1111/jfpp.16565

Wang, Z., Ding, Y., Deng, H., Yang, F., & Zhu, N. (2018). An Occupant-Oriented Calculation Method of Building Interior Cooling Load Design. *Sustainability*, *10*(6), 1821. https://doi.org/10.3390/su10061821

Watkins, M. W. (2018). Exploratory Factor Analysis: A Guide to Best Practice. *Journal of Black Psychology*, *44*(3), 219–246. https://doi.org/10.1177/0095798418771807

Yaddarabullah, A., Y. M., Rahman, A. B. A., & Saad, A. (2023). Measurement of Cooling Load-Based Occupant Behavior in Under-Actuated Zones: A Time-Variance Approach. *American Journal of Applied Sciences*, *20*(1), 48–64. https://doi.org/10.3844/ajassp.2023.48.64

Yan, D., O'Brien, W., Hong, T., Feng, X., Burak Gunay, H., Tahmasebi, F., & Mahdavi, A. (2015). Occupant Behavior Modeling for Building Performance Simulation: Current State and Future Challenges. *Energy and Buildings*, *107*, 264–278. https://doi.org/10.1016/j.enbuild.2015.08.032

Yang, D., Ngoc, K. M., Shin, I., & Hwang, M. (2023). DPReLU: Dynamic Parametric Rectified Linear Unit and Its Proper Weight Initialization Method. *International Journal of Computational Intelligence Systems*, *16*(1), 11. https://doi.org/10.1007/s44196-023-00186-w

Yang, T., Bandyopadhyay, A., O'Neill, Z., Wen, J., & Dong, B. (2022). From Occupants to Occupants: A Review of the Occupant Information Understanding for Building HVAC Occupant-Centric Control. *Building Simulation*, *15*(6), 913–932. https://doi.org/10.1007/s12273-021-0861-0

Yang, Z., & Becerik-Gerber, B. (2016). How Does Building Occupancy Influence Energy Efficiency of HVAC Systems? *Energy Procedia*, *88*, 775–780. https://doi.org/10.1016/j.egypro.2016.06.111

Zhang, T., Zhu, T., Xiong, P., Huo, H., Tari, Z., & Zhou, W. (2020). Correlated Differential Privacy: Feature Selection in Machine Learning. *IEEE Transactions on Industrial Informatics*, *16*(3), 2115–2124. https://doi.org/10.1109/tii.2019.2936825

Zhang, Z. (2024). Application of ARIMA and LSTM Model to the Forecast of CSI 300 Close Price. *Highlights in Science, Engineering and Technology*, *88*, 174–181. https://doi.org/10.54097/0929np93

Zhao, L., Li, Y., Liang, R., & Wang, P. (2022). A State of Art Review on Methodologies of Occupancy Estimating in Buildings from 2011 to 2021. *Electronics*, *11*(19), 3173. https://doi.org/10.3390/electronics11193173